ARTICLES

Unusually Large Dynamic Electron Polarization in an $O_2(^1\Delta_g)$−2,2,6,6-Tetramethylpiperidine-1-oxyl Radical System

Masaaki Mitsui,[†,‡] Keizo Takeda,[†] Yasuhiro Kobori,[†,§] Akio Kawai,[*,†] and Kinichi Obi[†,||]

Department of Chemistry, Graduate School of Science and Engineering, Tokyo Institute of Technology, 2-12-1 Ohokayama, Meguro-ku, Tokyo 152-8551, Japan, Department of Chemistry, University of Chicago, 5735 South Ellis Avenue, Chicago, IL 60637-1403, and Department of Chemical and Biological Sciences, Japan Women's University, 2-8-1 Mejirodai, Bunkyo-ku, Tokyo 112-8681, Japan

Received: May 6, 2003; In Final Form: November 14, 2003

Net absorptive (Abs) chemically induced dynamic electron polarization (CIDEP) is observed in the system of the lowest excited singlet molecular oxygen $O_2(^1\Delta_g)$ and 2,2,6,6-tetramethylpiperidine-1-oxyl (TEMPO) radical in benzene by means of the time-resolved ESR (TR-ESR) spectroscopy. As a result of (1) the analysis of CIDEP time profiles by the modified Bloch and kinetic equations and (2) the quenching of CIDEP by triethylamine, it is confirmed that the Abs CIDEP is created through the interaction of $O_2(^1\Delta_g)$ with TEMPO. The creation of Abs CIDEP is reasonably interpreted in terms of the radical-triplet pair mechanism (RTPM) of the $O_2(^3\Sigma_g^-)$−TEMPO pair with doublet precursor. The absolute magnitude of net Abs CIDEP created on TEMPO is experimentally estimated to be 340 ± 40 in the unit of Boltzmann polarization. To our knowledge, this is one of the largest magnitudes of CIDEP measured so far by the TR-ESR method. Based upon the RTPM theory, the origin of this unusually large CIDEP is attributed to the large spin relaxation effect via the electron spin dipole−dipole interaction of $O_2(^3\Sigma_g^-)$ formed in the quenching process of $O_2(^1\Delta_g)$ by TEMPO. As a result of the discussion about the large CIDEP in $O_2(^1\Delta_g)$ quenching by TEMPO, it is proposed that the quenching takes place through the enhanced intersystem crossing accompanied with strong electron exchange interaction between an oxygen molecule and a TEMPO radical.

1. Introduction

$O_2(^1\Delta_g)$ is one of the activate oxygen species and its chemical and physical processes have been extensively investigated over the last four decades.[1−3] $O_2(^1\Delta_g)$ plays an important role in physiological processes,[2] in organic synthesis, in photodegradation of polymers, and so on.[3] In particular, $O_2(^1\Delta_g)$ is of great use in recently developing photodynamic therapy for cancer.[2b] To understand $O_2(^1\Delta_g)$ chemistry in various situations, time-resolved $O_2(^1\Delta_g)$ detection methods such as measurements of IR phosphorescence, thermal lensing, and the quencher bleaching are very important and have been widely used.[1c] These methods were applied to the study of $O_2(^1\Delta_g)$ dynamics and its reactivity with other molecules, even with free radicals.[4,5] Recently, a time-resolved ESR (TR-ESR) detection of chemically induced dynamic electron polarization (CIDEP) of stable nitroxide radicals has been developed as another $O_2(^1\Delta_g)$ detection method.[6,7] Previously, we have for the first time found that CIDEP giving a net enhanced absorption (Abs) ESR signal is produced through the interaction between an $O_2(^1\Delta_g)$ and a 2,2,6,6-tetramethylpiperidine-1-oxyl (TEMPO) radical.[6a] Understanding of this useful CIDEP was easily done because of a number of previous TR-ESR experiments about CIDEP generated through interactions between an excited molecule and a free radical.[6,8−15] At present, this phenomenon has been well explained by the radical−triplet pair mechanism (RTPM). According to RTPM, the RT pair with quartet (Q) and doublet (D) states are selectively formed through the encounter of triplet and singlet excited molecules and a radical, respectively.[8−10] In our previous study, the net Abs CIDEP in the $O_2(^1\Delta_g)$−TEMPO system is interpreted by RTPM of the $O_2(^3\Sigma_g^-)$−TEMPO pair with doublet precursor. This CIDEP enhances the transient ESR signal which enables us to measure the time evolution of the $O_2(^1\Delta_g)$ concentration with a good signal-to-noise (S/N) ratio and to determine the decay rate of $O_2(^1\Delta_g)$.[6a,6d]

Beside a development of the new technique, this experimental finding opens a novel possibility to investigate the fast reaction dynamics of $O_2(^1\Delta_g)$ with radicals by analyzing the CIDEP pattern using the TR-ESR method. So far, there are only a few time-resolved studies on the reaction mechanism of $O_2(^1\Delta_g)$ with free radicals.[4,5] All of these studies have been performed by optical measurements. For example, Darmanyan and Tatikolov[4] studied the quenching of $O_2(^1\Delta_g)$ luminescence at 1270 nm by nitroxide radicals in the liquid phase and reported that the quenching takes place with small rate constants ($10^5 \sim 10^7$ s^{-1}) through the enhanced intersystem crossing (E-ISC). The CIDEP

* To whom correspondence should be addressed. E-mail: akawai@chem.titech.ac.jp. Phone: +81-3-5734-2231. Fax: +81-3-5734-2655.
† Tokyo Institute of Technology.
‡ Present address: Department of Chemistry, Keio University, 3-14-1 Hiyoshi, Kohoku-ku, Yokohama, Kanagawa 223-8522, Japan.
§ Present address: University of Chicago.
|| Present address: Japan Women's University.

10.1021/jp035235m CCC: $27.50
Published on Web 01/24/2004

generated via RTPM is directly related to the intermolecular dynamics in the encounter of an excited molecule with a free radical. Therefore, the CIDEP gives us more direct information of the intermolecular interactions between an excited molecule and a free radical than the conventional optical measurements. In this paper, a further investigation of the CIDEP generated in the $O_2(^1\Delta_g)$−TEMPO system was performed to understand the reaction dynamics of $O_2(^1\Delta_g)$ with a free radical. From the analysis of CIDEP time profiles based on the modified Bloch and kinetic equations, we estimated the absolute magnitude of net Abs CIDEP created at each encounter of $O_2(^1\Delta_g)$ with the TEMPO radical. As a result, it is found that a surprisingly large magnitude of net Abs CIDEP is created on TEMPO radicals. Finally, a theoretical analysis is carried out to rationalize the origin of unusually large CIDEP creation in the $O_2(^1\Delta_g)$−radical system.

2. Experimental Methods

TR-ESR Measurements. The TR-ESR measurements were carried out without field modulation to improve the time resolution. Transient ESR signals generated by pulsed laser irradiation were detected by a diode of a conventional X-band ESR spectrometer (Varian E−112 or Bruker, ELEXIS 580E) and accumulated by a boxcar integrator (Stanford SR-250) for spectra, or a transient memory (Tektronix TDS 350) for time profiles. The gate time width of the boxcar integrator and microwave power were suitably set in each measurement. An excitation light source was a XeCl excimer laser (Lambda Physik LPX 100) or a Nd:YAG laser (Continuum Powerlight 8000) with their power properly attenuated by series of filters. Sample solutions were flowed through a flat cell (0.5 mm interior space) in the ESR cavity. All measurements were carried out at ca. 300 K.

TR−Thermal Lensing Measurements. An excitation light source was the XeCl excimer laser (308 nm) or the Nd:YAG laser (532 nm). A He−Ne laser beam (NEG GLG-5380; 1.5 mW) used as an analyzing beam of TR-thermal lensing (TL) signals was focused in front of a sample cuvette (10 mm interior space) with a 70-mm focal length lens collinearly to the excitation laser pulse focused with a 200-mm focal length lens. The laser power was monitored by a silicon photodiode (Hamamatsu Photonics S1336−5BQ) calibrated with a pyroelectric detector (Gentec ED 100). The He−Ne laser beam sampled through a pinhole with 500 μm diameter and a monochromator (Nikon P-250) was detected by a photomultiplier tube (Hamamatsu R928). The output current was converted into voltage with a 500-Ω load register and digitized with a transient memory (Tektronix TDS 350). All measurements were carried out at ca. 300 K.

Materials. Anthracene and 9,10-dichloroanthracene (DCA) were recrystallized from GR grade benzene. Benzophenone (BP) and phenazine were recrystallized from GR grade *n*-hexane and ethanol, respectively. GR grade benzene was used as solvent without further purification. TEMPO and tetraphenylporphin (Aldrich) were used as received. All of the other chemicals were from Tokyo Kasei. Optical densities of sample solution were determined by a UV−vis spectrometer (Shimadzu UV2200).

3. Results and Discussions

3.1. Net Abs CIDEP in the O_2−TEMPO System. First of all, we overview the CIDEP creation in the $O_2(^1\Delta_g)$−TEMPO system briefly. Figure 1a shows TR-ESR spectrum obtained by the laser irradiation of anthracene in an anthracene/TEMPO mixture in air-saturated benzene, together with a CW-ESR

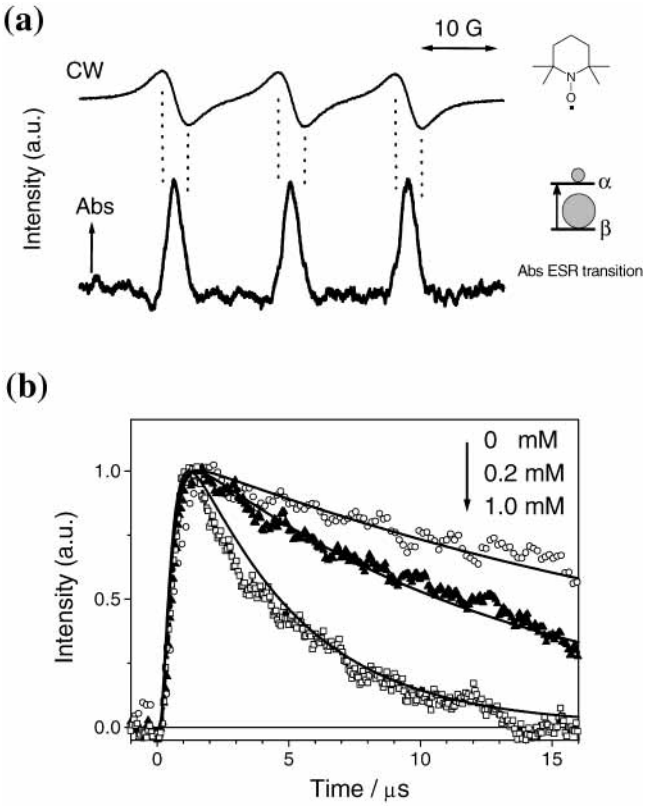

Figure 1. (a) CW and TR-ESR spectra of TEMPO obtained by the 355 nm laser excitation of the anthracene (7.0 mM)−TEMPO (3.0 mM) system in air-saturated benzene. The gate time was opened from 3 to 8 μs after the laser pulse. (b) ESR time profiles of TEMPO at $M_I = 0$ peak in the presence of TEA. TEA concentrations are 0 (circle), 0.8 (triangle), and 2.1 (rectangular) mM. The simulation curves were obtained by numerical analysis of Bloch and kinetic equations.

spectrum of TEMPO. The hyperfine structure coincides with that in the CW-ESR spectrum of TEMPO. The ESR signal pattern is Abs type, which means that β spin is enriched. Figure 1b shows time profiles of the TR-ESR signal at the $M_I = 0$ peak. The time evolutions are characterized by a simple rise and decay in Abs signal phase. No significant difference of the time evolution was found among the three hyperfine lines. In the air-saturated anthracene−TEMPO system, triplet anthracene is quenched by $O_2(^3\Sigma_g^-)$ and efficiently produces $O_2(^1\Delta_g)$ with $\Phi_\Delta = 0.61 \sim 0.88$.[16] Thus, the following scheme is considered:

$$S_0 + h\nu \rightarrow S_1 \xrightarrow{ISC} T_1 \quad (1)$$

$$T_1 + O_2(^3\Sigma_g^-) \rightarrow S_0 + O_2(^1\Delta_g) \quad (2)$$

$$O_2(^1\Delta_g) + R \xrightarrow{k_q^\Delta} {}^2(O_2(^3\Sigma_g^-)\cdots R) \rightarrow O_2(^3\Sigma_g^-) + {}^*R \quad (3)$$

$$O_2(^1\Delta_g) \xrightarrow{k_\Delta} O_2(^3\Sigma_g^-) \quad (4)$$

$$O_2(^1\Delta_g) + S_0 \xrightarrow{k_r} \text{product} \quad (5)$$

where S and T represent the singlet and the triplet states of anthracene, respectively. R denotes TEMPO and *R is a TEMPO radical which has quenched $O_2(^1\Delta_g)$ and possesses a certain amount of CIDEP. The k_q^Δ, k_Δ, and k_r are the rate constants of $O_2(^1\Delta_g)$ quenching by TEMPO, the unimolecular decay of $O_2(^1\Delta_g)$, and the chemical reaction of $O_2(^1\Delta_g)$ with anthracene, respectively. The net Abs CIDEP is created through

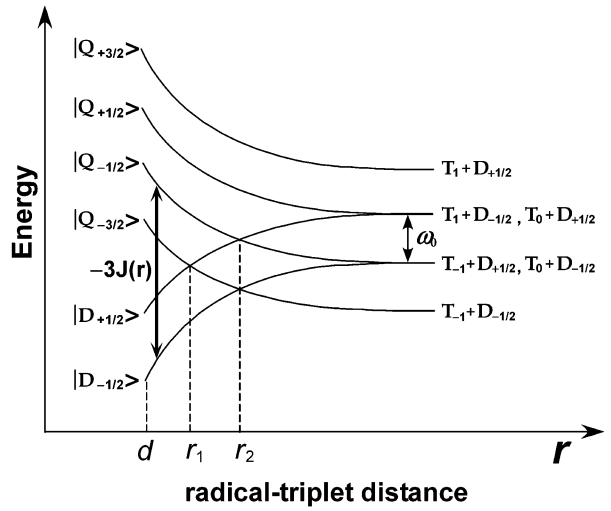

Figure 2. Energy diagram of the spin state of RT encounter complex along radical-triplet distance under the Zeeman energy of ω_0. The electron exchange interaction of radical-triplet pair is assumed to be negative (Q > D). T_i denotes the triplet states with magnetic quantum numbers, $i = 1$, 0, and -1, whereas D_i denotes the doublet states with $i = 1/2$ and $-1/2$.

the $O_2(^1\Delta_g)$−TEMPO interaction as described in reaction 3. We performed similar TR-ESR measurements with different sensitizers such as phenazine, tetraphenylporphrin, and DCA for $O_2(^1\Delta_g)$ production, and the net Abs CIDEP creation on TEMPO was identified in all of the systems examined. We note that the net Abs signal of TEMPO observed is not due to a Boltzmann polarization of TEMPO, because Boltzmann polarization of stable nitroxide radicals can hardly be detected by our diode detector with the preamplifier which eliminates the steady-state polarization as described by Turro et al.[17] The decay rate of CIDEP is governed by the $O_2(^1\Delta_g)$ lifetime. In the presence of $O_2(^1\Delta_g)$ quenchers such as triethylamine (TEA), the CIDEP decay rate increases as seen in Figure 1b because the $O_2(^1\Delta_g)$ lifetime becomes short as the quencher concentration increases.

There is a possibility that the deactivation of triplet anthracene by TEMPO, i.e.

$$T_1 + R \rightarrow S_0 + **R \qquad (6)$$

competes with reaction 2. However, the quenching rate constant of reaction 6 determined by the transient absorption method in this work is 1.2×10^7 M^{-1} s^{-1} (M = mol dm^{-1}) in benzene, which is two orders smaller than that of reaction 2 (i.e., 2.78×10^9 M^{-1} s^{-1} in benzene[18]). Besides, the concentration of O_2 in air-saturated benzene at 300 K (ca. 1.9 mM)[19] is close to that of R, i.e., [TEMPO] = 3.0 mM. This means that the rate of reaction 6 is two orders smaller than that of reaction 2. Thus, the process of (6) is negligible.

The CIDEP creation in the excited singlet molecule-radical system has been explained by the doublet precursor (DP)-RTPM.[9,10] Figure 2 shows the potential surfaces of spin states of RT pairs with exchange interaction, $-3J(r) = E(\text{quartet}) - E(\text{doublet})$. A negative sign of $J(r)$ is assumed because a positive $J(r)$ is unusual in RT pairs of organic compounds.[12] According to the DP−RTPM, E-ISC in the S_1 quenching is spin-selective and only D spin states of RT pairs $|D \pm 1/2\rangle$ are exclusively generated. Because there are no populations in Q states $|Q \pm 3/2\rangle$ and $|Q \pm 1/2\rangle$, the Q−D mixing in RT pairs starts from the D spin states. Consequently, the absorptive CIDEP is generated on radicals.[9,10] As shown in reaction 3, the RT pair, i.e., TEMPO−$O_2(^3\Sigma_g^-)$ pair, with doublet precursor is produced in the quenching process of $O_2(^1\Delta_g)$ by TEMPO. Therefore, the Abs CIDEP observed in the present system can be explained by the DP−RTPM.[6a]

3.2. Estimation of the Absolute Magnitude of CIDEP. The intensity of TR-ESR signal inherently depends on several factors such as the absolute magnitude of CIDEP (P_n), the quenching rate constant, and the spin relaxation time. In the $O_2(^1\Delta_g)$−TEMPO system examined here, the quenching of $O_2(^1\Delta_g)$ by TEMPO occurs with at very slow rate (e.g., $\sim 1.5 \times 10^3$ s^{-1} at [TEMPO] = 3.0 mM in toluene[6a]), and the spin−spin relaxation time of TEMPO is very short due to the dissolved oxygen molecules in solution. These facts would cause the large reduction of the signal intensity. However, the TR-ESR spectrum exhibits a relatively good S/N ratio as seen in Figure 1a. This seems to imply that the absolute magnitude of CIDEP in the $O_2(^1\Delta_g)$−TEMPO system, P_n^Δ is extremely large. Therefore, it is very interesting to measure the P_n^Δ value created by the O_2-$(^1\Delta_g)$−TEMPO interaction. To determine the P_n^Δ value, a standard system to cancel an apparatus function is required. Previously, we reported that a net Em CIDEP (α enriched population) of TEMPO in a BP−TEMPO system is created by the quartet-precursor (QP) RTPM through the quenching of ^{3}-BP* by TEMPO.[13] In this system, an absolute magnitude of net Em polarization, P_n^{BP}, at $M_I = 0$ peak of TEMPO has been quantitatively determined as −6.9 in the unit of the spin polarization of TEMPO at thermal equilibrium, P_{eq}.[8b,13] Thus, we use the time-profile of CIDEP in the BP−TEMPO system as a standard time profile and analyze CIDEP time profiles in the $O_2(^1\Delta_g)$−TEMPO system to obtain the P_n^Δ value.

Figure 3 shows TR-ESR time-profiles of TEMPO at $M_I = 0$ peak in a BP−TEMPO (0.5 mM) system in deaerated benzene under various laser powers. We simulated the CIDEP time profiles in the ^{3}BP*−TEMPO system on the basis of the QP−RTPM. The simulation is made by numerical integration of the relevant Bloch equations, modified with additional terms to allow for chemical kinetics[20]

$$\frac{dM_y}{dt} = -\frac{M_y}{T_2^R} + \omega_1 M_z \qquad (7)$$

$$\frac{dM_z}{dt} = -\omega_1 M_y - \frac{(M_z - P_{eq}[\text{TEMPO}])}{T_1^R} + P_n^{BP} k_q^{BP}[\text{TEMPO}][^3\text{BP*}] \qquad (8)$$

$$\frac{d[^3\text{BP*}]}{dt} = -(k_T^{BP} + k_q^{BP}[\text{TEMPO}] + k_{TT}^{BP}[^3\text{BP*}])[^3\text{BP*}] \qquad (9)$$

where M_i represents the magnetization in the rotating frame, ω_1 is the microwave field amplitude, and T_1^R and T_2^R are the spin−lattice relaxation and the spin−spin relaxation times of TEMPO, respectively. The eq 8 for M_z contains coupling to M_y via ω_1, relaxation toward the equilibrium magnetization, P_{eq}-[TEMPO], and creation of M_z via the QP−RTPM. As mentioned above, a Boltzmann polarization of TEMPO cannot be detected in our TR-ESR measurements. Thus, we regard the M_y value created by the equilibrium magnetization, P_{eq}[TEMPO], as a baseline of CIDEP time profiles. The k_T^{BP} is a unimolecular decay rate, and k_q^{BP} and k_{TT}^{BP} are the rate constants for quenching by TEMPO and triplet−triplet annihilation, respectively. The kinetic constants of $k_T^{BP} = 1.5 \times 10^5$ s^{-1} and $k_q^{BP} = 2.0 \times 10^9$ M^{-1} s^{-1} in the literature[21] were used in the analysis. The k_{TT}^{BP}

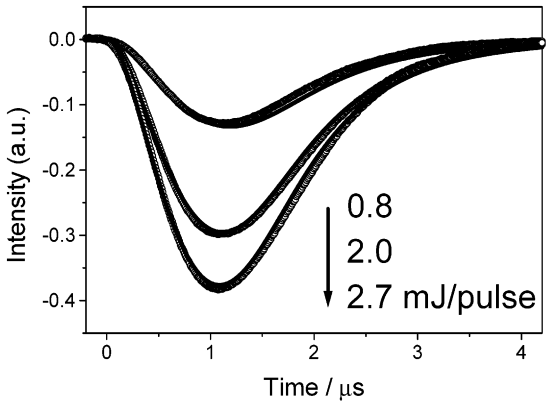

Figure 3. ESR time profiles (open circle) of TEMPO in the system of BP−TEMPO (0.5 mM) in deaerated benzene under various laser powers depicted in the figure. The signals were measured at the $M_I = 0$ peak with a microwave power of 5 mW. The optical density of BP is 0.18 at 355 nm. Simulation curves (solid lines) were obtained by the estimated initial triplet BP concentrations of 0.052, 0.13, and 0.18 mM for laser powers of 0.8, 2.0, and 2.7 mJ/pulse, respectively.

value of 1.0×10^{10} $M^{-1}s^{-1}$ which is the diffusion rate constant in benzene is assumed because triplet−triplet annihilation is diffusion controlled process.[22] The T_2^R value at [TEMPO] = 0.5 mM in deaerted benzene was calculated to be 50 ns from the line-width of CW-ESR spectrum. The reported T_1^R value is 250 ns in deaerated benzene.[11b,14] The ω_1 value for our ESR cavity was measured to be about 9.5×10^5 rad/s at incident power of 5 mW. The time-response function of our ESR system calibrated previously is also considered in the simulation. ESR signal intensity is related to the M_y value multiplied by apparatus function. Therefore, we determine the apparatus function from a set of the best-fitted simulation curves shown in Figure 3. The simulation well reproduces the observed time evolutions with a unique value of apparatus function.

Next, we examined the CIDEP time profiles in the $O_2(^1\Delta_g)$−TEMPO system. The simulation was also made by a numerical integration of the modified Bloch equations similar to eqs 7−9. In the $O_2(^1\Delta_g)$−TEMPO system, eqs 8 and 9 are respectively replaced by the following equations:

$$\frac{dM_z}{dt} = -\omega_1 M_y - \frac{(M_z - P_{eq}[\text{TEMPO}])}{T_1^R} + P_n^\Delta k_q^\Delta [\text{TEMPO}][O_2(^1\Delta_g)] \quad (10)$$

$$\frac{d[O_2(^1\Delta_g)]}{dt} = -\left(k_q^\Delta [\text{TEMPO}] + k_r^{DCA}[\text{M}] + \frac{1}{\tau_\Delta}\right)[O_2(^1\Delta_g)] \quad (11)$$

The τ_Δ and k_r^{DCA} are the $O_2(^1\Delta_g)$ lifetime in benzene and a reaction rate with DCA. The T_2^R values were estimated from the line-width of CW-ESR spectra and the T_1^R value of about 250 ns at $M_I = 0$ is used.

Because the kinetic parameters are significantly important for accurate determination of the P_n^Δ value, we measured the values by TR-TL method in the present study. The value of k_q^Δ is directly involved in the CIDEP creation term in eq 10 and is the most important value. Although we have already determined the k_q^Δ value in toluene previously,[6a] we need the k_q^Δ in benzene for the present study. The BP−TEMPO system used as a standard system for our apparatus is in benzene. This is because triplet BP usually undergoes hydrogen abstraction reaction with

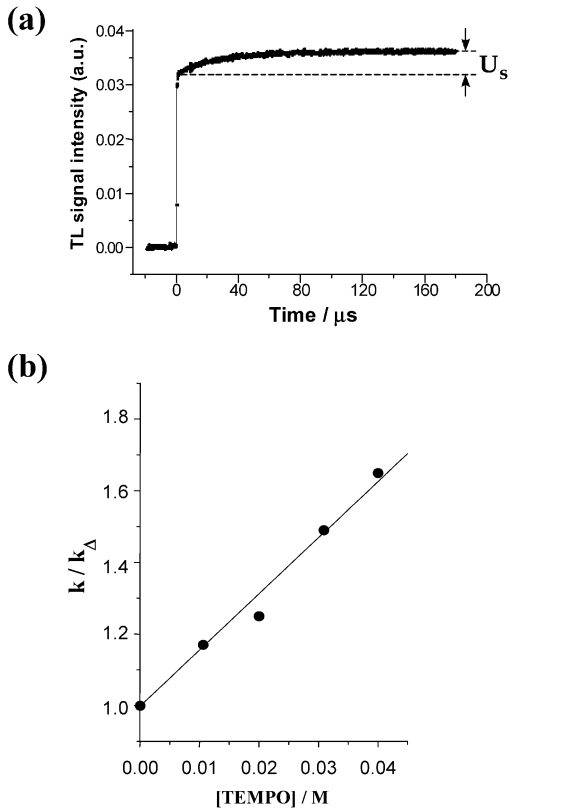

Figure 4. (a) Typical temporal profile of the TR-TL signal in the DCA (0.5 mM)-TEMPO (0.2 mM) system in benzene under air-saturated condition. (b) Plots of the decay rate constant of $O_2(^1\Delta_g)$ against TEMPO concentration measured by TR-TL method.

the solvent, and thus, it is necessary to use a solvent such as benzene which is chemically stable with triplet BP. Figure 4a shows a typical time evolution of the TL signal in a DCA−TEMPO system. The signal rises promptly and then slowly as described by U_S. The fast-rising part comes from a heat due to the fast radiationless transitions such as internal conversion and ISC of ^{1}DCA* and energy transfer (^{3}DCA* + $O_2(^3\Sigma_g^-) \rightarrow$ DCA + $O_2(^1\Delta_g)$). The energy transfer is very efficient and is nearly a diffusion controlled reaction.[21] The slow-rising part reflects the heat due to E-ISC and unimolecular ISC of O_2 ($^1\Delta_g \rightarrow {}^3\Sigma_g^-$). This assignment is confirmed by the fact that the slow-rising part in the absence of TEMPO is represented by a single-exponential decay with a rate of 3.45×10^4 s^{-1}, i.e., 29 μs, which agrees with the literature $O_2(^1\Delta_g)$ lifetime value of 30 μs.[21] Thus, the single-exponential fitting was applied to the slow decay component, and the decay rate constants of $O_2(^1\Delta_g)$ at various concentrations of TEMPO were determined. The observed first-order rate constants for $O_2(^1\Delta_g)$ decay were plotted against the TEMPO concentration as given in Figure 4b. From the least-squares fit of the data, k_q^Δ was determined to be $(5.7 \pm 0.2) \times 10^5$ M^{-1} s^{-1} in benzene. Similarly, we also determined the k_r^{DCA} value as $(1.3 \pm 0.2) \times 10^5$ M^{-1} s^{-1} in benzene by the TR-TL method.

According to these kinetic values, we simulated the ESR time evolution curves. In the beginning, we tried to simulate the time evolution curves in Figure 1b. The k_r value with anthracene in the literature[1b] of 8.5×10^5 M^{-1} s^{-1} was used in the simulation. The quenching rate constant, k_q^{TEA} of $O_2(^1\Delta_g)$ by TEA was the only parameter and the best simulation was obtained with $k_q^{TEA} = 2 \times 10^8$ $M^{-1}s^{-1}$. This value was close to the k_q^{TEA} of 3×10^8 $M^{-1}s^{-1}$ determined by the TR-TL method in this study. This

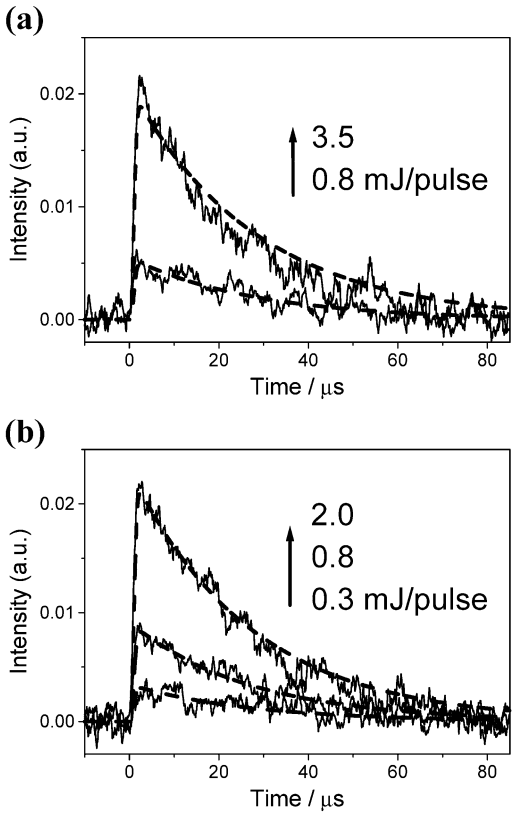

Figure 5. Time profiles (solid lines) of the ESR signal of TEMPO in the system of DCA(1.4 mM)−TEMPO in air-saturated benzene under various laser powers. TEMPO concentrations are (a) 1.8 and (b) 4.0 mM. The signals were measured at the $M_I = 0$ peak with a microwave power of 5mW. An optical density of DCA is 0.24 at 355 nm. Simulation curves (dotted lines) were obtained by the estimated initial ^{1}*DCA concentrations of 0.020, 0.052, 0.13, and 0.23 mM for laser powers of 0.3, 0.8, 2.0, and 3.5 mJ/pulse, respectively. T_2^R values used in the simulations are (a) 21.4 and (b) 17.5 ns which were obtained by the line-width analysis of CW-ESR spectra of TEMPO. The P_n^Δ values in units of P_{eq} obtained by the simulations are (a) 360 ± 90 and 320 ± 70 for 0.8 and 3.5 mJ/pulse, respectively and (b) 340 ± 140, 340 ± 50, and 350 ± 30 for 0.3, 0.8, and 2.0 mJ/pulse, respectively.

simulation demonstrates that the time evolution can be analyzed by the present procedure.

Finally, the analysis of CIDEP time profiles in the $O_2(^1\Delta_g)$−TEMPO system were performed with the apparatus function determined by the simulations shown in Figure 3. Figure 5, parts a and b, shows time evolution curves of CIDEP in the $O_2(^1\Delta_g)$−TEMPO system under various laser powers and TEMPO concentrations. Other experimental conditions (i.e., laser alignment, signal sensitivity, and microwave power) were the same in the BP−TEMPO (Figure 3) and the $O_2(^1\Delta_g)$−TEMPO (Figure 5) systems. We adjusted the concentration of DCA so as to produce the same initial concentration of the excited triplet BP (^{3}BP*) in Figure 3 and the lowest excited singlet molecular oxygen, $O_2(^1\Delta_g)$, in Figure 5 as far as the same laser power is used. For this procedure, it is necessary to find the ISC quantum yields of BP and DCA and the quantum yield of $O_2(^1\Delta_g)$ formation (Φ_Δ) by DCA in benzene. The former values are 1.0 and 0.91 in the literature, respectively.[19] The latter is 0.82 ± 0.02, which was determined by utilizing the TR-TL method in this work. The optical density of BP used in Figure 3 is 0.18 at 355 nm for the 0.5 mm interior cell. Thus, we prepared the DCA sample solutions with an optical density at 0.24. The best fitting curves for each time profile were obtained as shown in Figure 5, parts a and b. As the final result, the P_n^Δ value was determined to be (340 ± 40) P_{eq} by using the reported value of $P_n^{BP} = -6.9\ P_{eq}$.[14] It is interestingly noted that P_n^Δ value is comparable to the upper limit value of net RTPM polarization,[14] i.e., 670 P_{eq} and much larger than the reported P_n values of the triplet organic molecule-TEMPO systems (<10 P_{eq}).[11,13−15] In general, P_n values of radicals involved in photochemical processes are on the order of 10 P_{eq} or less in low viscosity solvents such as benzene and toluene.[11,13,14,15,23] To the best of our knowledge, the P_n^Δ value is one of the largest magnitudes of CIDEP measured so far by the TR-ESR method.

It is noteworthy that the S/N ratio of time profiles of the O_2-($^1\Delta_g$)−TEMPO system are much lower than those of the BP−TEMPO system (see Figure 3), though the absolute magnitude of CIDEP in the $O_2(^1\Delta_g)$−TEMPO system is much larger. One of probable reasons is a quite low quenching efficiency (Φ_q) of $O_2(^1\Delta_g)$ by TEMPO, i.e.

$$\Phi_q^\Delta = \frac{k_q^\Delta[\mathrm{TEMPO}]}{k_\Delta + k_r[\mathrm{M}] + k_q^\Delta[\mathrm{TEMPO}]} \le 0.05 \qquad (12)$$

which is much lower than that of ^{3}BP* by TEMPO, i.e.

$$\Phi_q^{BP} = \frac{k_q^{BP}[\mathrm{TEMPO}]}{k_T + k_q^{BP}[\mathrm{TEMPO}]} \approx 0.87 \qquad (13)$$

Another reason is that the T_2^R value in the $O_2(^1\Delta_g)$−TEMPO system is much shorter than that of BP−TEMPO system. As mentioned above, these factors largely reduce the TR-ESR signal intensities at each peak of hyperfine lines in the $O_2(^1\Delta_g)$−TEMPO system irrespective of the quite large absolute magnitude of CIDEP. In the case of a radical having a higher quenching efficiency of $O_2(^1\Delta_g)$, a much larger TR-ESR signal would be observed.

3.3. Theoretical Consideration. It is very intriguing to elucidate the origin of the extremely large CIDEP generation in this system by comparing the experimental value with ones obtained by a theoretical calculation. Adrian has proposed[24] the linearly varying model and expressed the formula in the strong exchange interaction limit, $3J_0 \gg \omega_0$ where $-3J_0$ is the exchange interaction at the closet approach and ω_0 is the Zeeman energy. In this model, the Q−D mixing by anisotropic zfs interaction due to electron spin dipoles in the triplet molecule is important around the level crossing regions ($r \approx r_1, r_2$). Kobori et al.[14] utilized this formula and express the absolute magnitude of net CIDEP by RTPM polarization as follows:

$$P_n = \frac{1}{135}\mathrm{sign}(J_0)\frac{{D_{zfs}}^2}{\omega_0 \alpha D_r}\{r_1 \arctan(2\omega_0 \cdot \tau_c) + 4r_2 \arctan(\omega_0 \cdot \tau_c)\} \qquad (14)$$

where τ_c is the correlation time and D_r is the diffusion constant in the solvent. The α is a parameter used in the usual form of an exponentially decaying exchange interaction

$$J(r) = J_0 \exp\{-\alpha (r - d)\} \qquad (15)$$

where d is the distance of the closest approach in RT pair.

On the other hand, Shushin[25] proposed another theoretical model, i.e., the relaxational mechanism, where all couplings between Q and D spin states are considered and the net CIDEP is created on free radicals by the Q−D transitions induced by the fluctuating zfs interaction of triplet molecule. In the strong

TABLE 1: Absolute Magnitudes of Net Abs CIDEP of TEMPO Observed (obs.) and Calculated (calc.) for the $O_2(^1\Delta_g)$−TEMPO System in Benzene Solution at Room Temperature (in Units of Boltzmann Polarization)

P_n^Δ (obs.)	P_n^Δ (calc.)[a]	P_n^Δ (calc.)[b]
340 ± 40	1040[a]	740[b]

[a,b] Calculated by (a) eq 14 and (b) eq 16. The parameters used are, $3J_0e^{\alpha d} = -5.5 \times 10^{14}$ (rad/s), $\alpha = 1.4$ (Å^{-1}), $D_r = 8.2 \times 10^{-5}$ (cm/s^2), and $\tau_c = 4$ (ps).

exchange interaction limit ($3J_0 \gg \omega_0$), the formula for the magnitude of net CIDEP by RTPM is given by[25a]

$$P_n = \frac{\pi}{45}\frac{{D_{zfs}}^2}{{\omega_0}^2}\frac{\omega_0 d}{\alpha D_r}\left(\frac{1}{1+(\omega_0 \cdot \tau_c)^2} + \frac{4}{4+(\omega_0 \cdot \tau_c)^2}\right) \quad (16)$$

In this theoretical formula, it is assumed that the RT pair is initially produced at the distance of the closest approach. Both eqs 14 and 16 were derived under the short correlation time approximation, and no back transitions between Q and D spin states are considered.[24,25] These formulas can be applied under the nonviscous condition ($\omega_0\tau_c < 1$). To calculate the P_n^Δ values from eqs 14 and 16, we used the following parameters: Zeeman splitting obtained from the microwave counter ($\omega_0 = 6.0 \times 10^{10}$ rad/s under the present X-band ESR experimental condition) and the reported D_{zfs} value[26] of 7.53×10^{11} rad/s ($= 3.96$ cm^{-1}) for $O_2(^3\Sigma_g^-)$. D_r of O_2 in benzene at room temperature has been reported to be 5.7×10^{-5} cm^2/s,[27] and that of TEMPO was assumed to be 2.5×10^{-5} cm^2/s at room temperature[13,14] (and, thus, additionally $D_r = 8.2 \times 10^{-5}$ cm^2/s). The correlation time τ_c is assumed to be 4 ps. The parameters in the exchange interaction of the $O_2(^3\Sigma_g^-)$−TEMPO pair were assumed to be on the same order of the magnitude with those in the transient radical pairs. Thus, we put $3J_0e^{\alpha d} = -5.5 \times 10^{14}$ rad/s, $\alpha = 1.4$ Å^{-1}, and $d = 4$ Å. This gives the separations between the TEMPO and $O_2(^3\Sigma_g^-)$ at the level crossing of $r_1 = 7.2$ Å and $r_2 = 7.7$ Å from eq 15. As the final result, the absolute magnitudes of CIDEP created on TEMPO in the $O_2(^1\Delta_g)$−TEMPO system were calculated as 1040 P_{eq} and 740 P_{eq} respectively by eqs 14 and 16. P_n^Δ values determined experimentally and theoretically are summarized in Table 1.

Both models predict that the extremely large magnitude of CIDEP can be created on TEMPO in the $O_2(^1\Delta_g)$-TEMPO system. This is apparently due to the very large zfs constant (3.96 cm^{-1}) of $O_2(^3\Sigma_g^-)$ which highly accelerates the D−Q mixing. However, both predicted values of P_n^Δ are larger than the experimental value and exceed the upper limit of net polarization (i.e., 670 P_{eq}). Kobori et al. studied the viscosity dependence on the magnitude of net CIDEP in 1-chloronaphthalene−TEMPO system by changing the temperature.[14] They predicted that the back transition between Q and D spin states should simultaneously occur under viscous conditions ($\eta > 20$ cp) where the magnitude of net CIDEP amounts to 300 P_{eq}. This suggests that back transitions from the Q to the D spin states may also occur in the $O_2(^1\Delta_g)$-TEMPO system. In the two models applied here, however, only one-side Q−D transitions are considered; namely, D → Q transitions exclusively occur and Q → D type back-transitions are neglected.[24,25a] Thus, this may be a reason both models predict the larger values (which exceed the upper limit of net polarization) than the experimental one. In most of the RT systems, it has been successfully explained that the net CIDEP by RTPM is predominately created around the level crossing regions ($r \approx r_1, r_2$).[14] However, it appears that this picture is not suitable for the $O_2(^1\Delta_g)$−radical system, because the zfs constant of $O_2(^3\Sigma_g^-)$ is ca. 13 times larger than the Zeeman energy at the X-band ESR measurement. This large zfs interaction of $O_2(^3\Sigma_g^-)$ allows all of the Q and D spin states for coupling with one another not only around the level crossing regions but also in the wide range of regions.

3.4. $O_2(^1\Delta_g)$−TEMPO Reaction Dynamics. Darmanyan et al.[4] pointed out that neither the energy transfer nor the CT mechanisms[28] are responsible for the quenching of $O_2(^1\Delta_g)$ by nitroxide radicals because both the D_1 energy of nitroxide and predicted CT levels of $^2(O_2^- \cdots {}^{1or3}R^+)$ lie higher than that of the $^1\Delta_g$ state. Furthermore, the quenching rate constant does not increase sharply with solvent polarity. They have thereby concluded that only the electron exchange interaction leading to E-ISC is responsible for $O_2(^1\Delta_g)$ quenching by nitroxide radicals. However, they did not present any direct experimental evidence showing that there is intermolecular exchange interaction between molecular oxygen and nitroxide radical. In the present study, the large magnitude of CIDEP can be explained by assuming that the exchange interaction of the $O_2(^3\Sigma_g^-)$−TEMPO pair is much larger than the Zeeman energy (6.0×10^{10} rad/s). If the exchange interaction is weak ($3J_0 \ll \omega_0$), the predicted value of P_n^Δ should be very small. According to the formula for the weak exchange interaction case proposed by Shushin,[25a] P_n^Δ value for $3J_0 = 0.01 \times \omega_0$ is calculated to be ca. 5 P_{eq}. This is far less than the experimental value. The extremely large CIDEP magnitude evidently demonstrates that the $O_2(^3\Sigma_g^-)$−TEMPO pair is generated in the strong exchange interaction regions (i.e., region of $r < r_1, r_2$ in Figure 2). Namely, the quenching of $O_2(^1\Delta_g)$ by TEMPO takes place through E-ISC with the exchange interaction between them.

4. Concluding Remarks

We have observed the net Abs CIDEP on TEMPO in an $O_2(^1\Delta_g)$−TEMPO system in benzene by means of TR-ESR. From the simulation of the ESR time profile and the $O_2(^1\Delta_g)$ quenching experiment, we confirmed that net Abs CIDEP is created through the interaction of an $O_2(^1\Delta_g)$ with a TEMPO radical. The CIDEP mechanism was interpreted by the RTPM of an $O_2(^3\Sigma_g^-)$−radical encounter pair with doublet precursor. The absolute magnitude of CIDEP generated in the $O_2(^1\Delta_g)$−TEMPO system was experimentally estimated. Consequently, it was revealed that the surprisingly large CIDEP is created on TEMPO radicals through the interaction with $O_2(^3\Sigma_g^-)$ formed in the $O_2(^1\Delta_g)$ quenching process. Based upon the RTPM theories, the origin of the extremely large CIDEP created in the $O_2(^1\Delta_g)$−TEMPO system was attributed to the large zfs interaction of $O_2(^3\Sigma_g^-)$ which highly accelerates the D−Q state mixing. Finally, we revealed that the mechanism of $O_2(^1\Delta_g)$ quenching by nitroxide radicals is E-ISC induced by a strong electron exchange interaction in an encounter collision complex.

Because the first phosphorescence detection of $O_2(^1\Delta_g)$ was reported by Khan and Kasha,[29] most of the kinetic studies of $O_2(^1\Delta_g)$ have been owing to the time-resolved detection of $O_2(^1\Delta_g)$ phosphorescence[1] though the sensitivity in this method is not always high due to the relatively low sensitivity of the Ge diode detector or interference of other luminescence coexisting in the sample. Recently, a detection of $O_2(^1\Delta_g)$ in *vivo* has attracted much interest[30] and a position sensitive detection method has been required. The present method of $O_2(^1\Delta_g)$ detection by CIDEP measurement utilizes TEMPO radical as a sort of $O_2(^1\Delta_g)$ sensor without any chemical reaction. Once

TEMPO radical was successfully doped at a position where O_2-($^1\Delta_g$) physics and chemistry are of interest, CIDEP of the TEMPO radical could be used as a position sensitive detector of $O_2(^1\Delta_g)$. For application of CIDEP for this purpose, a sensitivity should be increased by more efforts to find better sensor molecules, $O_2(^1\Delta_g)$ sensitizers, EPR cavity and sample cell designs and so on. The absolute magnitude of CIDEP is quite important when we build a new $O_2(^1\Delta_g)$ detection system and thus, it is necessary to obtain P_n^{Δ} values of other free radicals. Measurements of these values are now in progress.

Acknowledgment. This work was supported in part by a Grant-in-Aid for Scientific Research (Nos. 13740327 and 15550005) from the Ministry of Education, Science, Culture and Sports of Japan.

References and Notes

(1) For examples, see: (a) Frimer, A. A., Ed.; *Singlet O_2*; CRC Press: Boca Ration, FL, 1985; Vols. 1−4. (b) Wilkinson, F.; Helman, W. P.; Ross, A. B. *J. Phys. Chem. Ref. Data.* **1995**, 24, 663. (c) Schweitzer, C.; Schmidt, R. *Chem. Rev.* **2003**, *103*, 1685.

(2) (a) Foote, C. S. *Free radicals in biology*; Pryor, W. A., Ed.; Academic Press: New York, 1976; pp 85−133. (b) Bonnett, R. *Chem. Soc. Rev*. **1995**, 19.

(3) (a) Pospisil, J., Klemchuk, P. P., Eds.; *Oxidation inhibition in organic materials*; CRC Press: Boca Raton, FL, 1990. (b) Clennan, E. L. *Tetrahedron*, **2000**, *56*, 9151. (c) DeRosa, M. C.; Crutchley, R. J. *Coord. Chem. Rev.* **2002**, *233*−*234*, 351.

(4) Darmanyan, A. P.; Tatikolov, A. S. *J. Photochem.* **1986**, *32*, 157.

(5) (a) Darmanyan, A. P.; Foote, C. S. *J. Phys. Chem.* **1995**, *99*, 11854. (b) Darmanyan, A. P.; Gregory, D. D.; Guo, Y.; Jenks, W. S.; Burel, L. B.; Eloy, D.; Jardon, P. *J. Am. Chem. Soc*. **1998**, *120*, 396. (c) Vidoczy, T.; Baranyai, P. *Helv. Chem. Acta* **2001**, *84*, 2640.

(6) (a) Mitsui, M.; Takeda, K.; Kobori, Y.; Kawai, A.; Obi, K. *Chem. Phys. Lett.* **1996**, *262*, 125. (b) Kawai, A.; Mitsui, M.; Kobori, Y.; Obi, K. *Appl. Magn. Reson.* **1997**, *12*, 405. (c) Fujisawa, J.; Ohba, Y.; Yamauchi, S. *J. Phys. Chem A*, **1997**, *101*, 434. (d) Kawai, A. *Appl. Magn. Reson.* **2003**, *23*, 349.

(7) Batchelor, S. N. *J. Phys. Chem. B* **1999**, *103*, 6700.

(8) (a) Blättler, C.; Jent, F.; Paul, H. *Chem. Phys. Lett.* **1990**, *166*, 375. (b) Kawai, A.; Okutsu, T.; Obi, K. *J. Phys. Chem.* **1991**, *95*, 9130. (c) Kawai, A.; Obi, K. *J. Phys. Chem.* **1992**, *96*, 5701.

(9) (a) Kawai, A.; Obi, K. *J. Phys. Chem.* **1992**, *96*, 52. (b) Kobori, Y.; Kawai, A.; Obi, K. *J. Phys. Chem.* **1994**, *98*, 6425.

(10) Kawai, A.; Obi, K. *Res. Chem. Intermed.* **1993**, *19*, 865.

(11) (a) Goudsmit, G. H.; Paul, H.; Shushin, A. I. *J. Phys. Chem.* **1993**, *97*, 19243. (b) Goudsmit, G. H.; Paul, H.; *Chem. Phys. Lett.* **1993**, *208*, 73.

(12) (a) Kawai, A.; Shibuya, K.; Obi, K. *Appl. Magn. Reson.* **2000**, *18*, 343. (b) Kawai, A.; Watanabe, Y.; Shibuya, K. *Mol. Phys.* **2002**, *100*, 1225. (c) Kawai, A.; Shibuya, K. *J. Phys. Chem A* **2002**, *106*, 12305. (d) Kawai, A.; Watanabe, Y.; Shibuya, K. *Chem. Phys. Lett.* **2003**, *372*, 8.

(13) Kobori, Y.; Mitsui, M.; Kawai, A.; Obi, K. *Chem. Phys. Lett.* **1996**, *252*, 355.

(14) Kobori, Y.; Takeda, K.; Tsuji, K.; Kawai, A.; Obi, K. *J. Phys. Chem. A* **1998**, *102*, 5160.

(15) Blank, A.; Levanon, H. *J. Phys. Chem. A* **2000**, *104*, 794.

(16) (a) Terazima, M.; Tonooka, M.; Azumi, T. *Photochem. Photobiol*. **1991**, *54*, 59. (b) Rossbroich, G.; Garcia, N. A.; Braslavsky, S. E. *J. Photochem.* **1985**, *31*, 37. (c) Stevens, B.; Marsh, K. L.; Barltrop, J. A. *J. Phys. Chem.* **1981**, *85*, 3079.

(17) Turro, N. J.; Koptyug, V. I.; van Willigen, H.; McLauchlan, K. A. *J. Magn. Reson. A* **1994**, *109*, 121.

(18) Gijzemann, O. L. J.; Kaufmann, F.; Porter, G. *J. Chem. Soc., Faraday Trans. 2* **1973**, *69*, 727.

(19) Murov, S. L.; Carmichael, I.; Hug, G. L. *Handbook of photochemistry;* Marcel Dekker: New York, 1993.

(20) Verma, N. C.; Fessenden, R. W. *J. Phys. Chem.* **1976**, *65*, 2139.

(21) Scaiano, J. C. *Handbook of Organic Photochemistry Volume II*; CRC Press: Boca Raton, FL, 1989.

(22) Yekta, A.; Turro, N. J. *Mol. Photochem.* **1972**, *3*, 307.

(23) (a) Savitsky, A. N.; Paul, H.; Shushin, A. I. *J. Phys. Chem. A* **2000**, *104*, 9091. (b) Batchelor, S. N.; Shushin, A. I. *Appl. Magn. Reson.* **2002**, *22*, 47.

(24) Adrian, F. J. *Chem. Phys. Lett.* **1994**, *229*, 465.

(25) (a) Shushin, A. I. *Chem. Phys. Lett.* **1993**, *208*, 173. (b) Shushin, A. I. *J. Chem. Phys.* **1992**, *97*, 3171. (c) Shushin, A. I. *J. Chem. Phys.* **1993**, *99*, 8723. (d) Shushin, A. I. *Chem. Phys. Lett.* **1999**, *313*, 246.

(26) Kearns, D. R. *Chem. Rev.* **1971**, *71*, 395.

(27) Ware, W. R. *J. Phys. Chem.* **1962**, *66*, 455.

(28) (a) Ouannes, C.; Wilson, T. *J. Am. Chem. Soc*. **1968**, *90*, 9527. (b) Ogryzlo, E. A.; Tank, C. W. *J. Am. Chem. Soc.* **1970**, *92*, 5034. (c) Smith, W. F., Jr. *J. Am. Chem. Soc.* **1972**, *94*, 186.

(29) Khan, A. U.; Kasha, M. *J. Chem. Phys.* **1963**, *39*, 2105.

(30) Oelckers, S.; Ziegler, T.; Michler, I.; Roder, B. *J. Photochem. Photobiol. B: Biol.* **1999**, *53*, 121.